© Universiti Tun Hussein Onn Malaysia Publisher's Office

IJIE

Journal homepage: http://penerbit.uthm.edu.my/ojs/index.php/ijie
ISSN : 2229-838X e-ISSN : 2600-7916

The International Journal of Integrated Engineering

Fabrication Rutile-Phased TiO_2 Film with Different Concentration of Hydrochloric Acid Towards the Performance of Dye-Sensitized Solar Cell

A. Norazlina[1,2]*, F. Mohamad[1,2], A. Talib[1,2], M.K. Ahmad[1,2], N. Nafarizal[1,2], C.F. Soon[1,2], A.B. Suriani[3], M.H. Mamat[4], K. Murakami[5], M. Shimomura[5]

[1]Department of Electronic Engineering, Faculty of Electrical & Electronic Engineering, Universiti Tun Hussein Onn Malaysia, 86400, Parit Raja, Batu Pahat, Johor, MALAYSIA

[2]Microelectronics and Nanotechnology Shamsuddin Research Centre (MiNT-SRC) Universiti Tun Hussein Onn Malaysia, 86400, Parit Raja, Batu Pahat, Johor, MALAYSIA

[3]Nanotechnology Reserach Centre, Department of Physic, Faculty of Science & Mathematics, Universiti Pendidikan Sultan Idris, 35900 Tanjung Malim, Perak, MALAYSIA

[4]Nano-Electronic Centre, Faculty of Electrical Engineering, Universiti Teknologi Mara, 40450 Shah Alam, Selangor, MALAYSIA

[5]Department of Engineering, Graduate School of Integrated Science and Technology, Shizuoka University, 432-8011 Hamamatsu, Shizuoka, JAPAN

*Corresponding Author

DOI: https://doi.org/10.30880/ijie.2020.12.02.014
Received 29 December 2019; Accepted 27 January 2020; Available online 28 February 2020

Abstract: In this study, one-step hydrothermal method is demonstrated to synthesis TiO_2 double-layer structure by modifying the concentration of hydrochloric acid (HCl). The X-ray diffraction (XRD) pattern analysis suggested that the dominant peak is rutile phase. Interesting morphologies such as cauliflower, chrysanthemum flower or dandelion structures over the nanorods layer were revealed by FE-SEM images and showed substantial effects to the thin film performance. UV-vis absorption spectra of prepared TiO_2 film is in UV limitation with band gap energy (E_g) range from 2.57eV to 3.0eV. The optimum photoelectric conversion efficiency of DSSC is 42.5% that exhibited the efficiency of 6.41% for the sample synthesized using equal proportion of de-ionized water and HCl amount or in another word in accordance of ratio 1:1. These results serve as a guidance principle for preparing high quality DSSC thin film.

Keywords: DSSC, hydrothermal process, hydrochloric acid concentration, Rutile TiO_2, double-layer structure

1. Introduction

DSSCs have been broadly studied in the present time because they provide numerous advantages in producing relatively cheaper and more efficiency solar cells. DSSCs can be made-up by using economical cost materials and procedures differed to the manufacturing of conventional silicon–based solar cells. The core constituent of DSSC is a photoanode electrode typically FTO or ITO substrate that having a nanostructured oxide semiconductor, such as a TiO_2

*Corresponding author: azlina78.ahmad@gmail.com

layer, a sensitizer which is dye, a counter electrode that carrying a reduction electrocatalyst, usually nanoparticulate platinum (Pt) and an electrolyte with a redox couple *(Vaiciulis et al.*, 2012). Thus, many studied have made efforts to facilitate the electron transportation for the enhancement of the DSSCs photovoltaic performance by controlling the titania photoanode composition and structure.

TiO_2 is one type of semiconductor materials that attracts researchers to do the extensive study. The superior properties of nano TiO_2 are come from its low dimensionality and quantum size effect (Wang *et al*., 2014) and due to these, it is necessary to regulate the particle size, shape, and distribution of the prepared sample TiO_2 film. There are thirteen polymorphs known of TiO_2 (Liu *et al.*, 2015) but only three phases have been widely investigated including anatase (Dhas *et al*., 2011; Hossain *et al*., 2010), rutile *(Francis et al*., 2011; Li *et al*., 2009) and brookite (Arier & Tepehan, 2011; Zou *et al*., 2014). The anatase and rutile phases have tetragonal structure whereas orthorhombic structure belongs to brookite phase. Every phase of TiO_2 possesses a different band gap which is rutile 3.0eV, anatase 3.2eV and 3.3eV for brookite (Lin *et al*., 2013). Rutile is known as the most stable phase at high temperatures and is the effortless to recognise as thin films or pure crystals whereas anatase and brookite are both meta-stable at all temperatures and could change into rutile phase upon heat treatment (Apátiga *et al*., 2006; Iacomi *et al*., 2007). Having a large band gap property will make TiO_2 as a perfect metal oxide semiconductor preferentially in DSSCs.

A tremendous study has been conducted for the desired and controllable nanostructure including sol-gel process (Maheswari & Venkatachalam, 2015), hydrothermal (Cabral *et al.*, 2015; J. Li *et al.*, 2010), chemical bath deposition (Dhandayuthapani *et al.*, 2016), spray pyrolysis (Manoharan and Sridhar, 2012; Oja *et al.*, 2006) and anodization (Nishanthi *et al*., 2010). Among them, hydrothermal process is a facile, convenient and favourable method in control the size of grain, the morphology of particle, the crystalline phase, and the surface chemistry by adjusting the composition of solution, the growth temperature reaction, the pressure, the properties of solvent, the additives, and the time of ageing. Su and co-workers growth rutile TiO_2 nanorods structure by sol-hydrothermal method under various reaction times (Su *et al*., 2011). Ten hours reaction time was chosen because it has high surface area with good crystalline as photonanodes for DSSC study. They also studied the effect of the HCl concentration and found that 3M HCl is the best parameter to synthesis pure rutile nanorods TiO_2 structure.

Liu & Aydil outlined seven factors including the effect of temperature, growth time, substrate type, acidity medium, reactant, concentration and precursors that influenced in the hydrothermally growth of nanorods structure (Liu & Aydil, 2009). They concluded that equal amount volume of de-ionized water and HCl is favourable for well-aligned growth of TiO_2 nanorods. These proportions have been applied in tremendous researches to synthesis the well-aligned nanorods array (Pawar *et al.*, 2016). Yuxiang and team studied the effect of precursor concentration, the hydrothermal duration time and the reaction temperature in preparing TiO_2 nanorod arrays by hydrothermal method to control the morphologies and alignment of the nanostructure (Yuxiang *et al.*, 2010).

In this article, the demonstration of one step hydrothermal method to synthesis TiO_2 double layer structure of nanoflowers on nanorods morphology and the effect of HCl volume are studied and discussed. In some articles, the role of HCl as solvent (Jithin *et al.*, 2016) or chelating agent (Senain et al., 2010) are very crucial in the formation of desired structure and sometimes could be used to obtain the most stable rutile phase (Wang *et al.*, 2014) of TiO_2 material. It shows that the growth mechanism under different concentration of acidic medium has significant influences to the properties of the synthesized thin film.

2. Materials and Methods

2.1 Synthesis of Rutile TiO_2 Films

All the chemicals were graded analytically and used without further purification. Fluorine-doped tin oxide (FTO) glass (7Ω/sq) with a thickness of 2.0 mm was cut into the pieces of 1.5 × 2.5 cm in dimension as substrates. These substrates were cleaned ultrasonically in acetone followed by ethanol and lastly de-ionized water (18.2MΩ, Mili-Q Ultrapure) for 10 minutes, respectively. TiO_2 double-layer structure were deposited using one-step hydrothermal method (Ahmad *et al.*, 2016). In a typical synthesis, 80mL deionized water with variable concentrated hydrochloric acid (36.5%–38% by weight) in range 50mL to 110mL was stirred for 5 min before 5mL of titanium butoxide (TBOT) was dropped wisely using capillary tube and stirred for another 10 minutes. A clear mixed solution was loaded into a 300ml Teflon-lined stainless-steel autoclave where the substrates of FTO were placed horizontally against the Teflon wall with an active side facing upward. Then the autoclave was sealed completely for hydrothermal synthesis at 150°C for 10h in the hot air oven. After cooling down to room temperature, the substrates were taken out, rinsed thoroughly with de-ionized water and permitted to dessicate naturally in ambient air. The samples are denoted as 'TiO_2-HC*v*' where 'HC' is the abbreviation for acid hydrochloric and '*v*' is corresponded to HCl volume.

2.2 DSSC Preparation

For the efficiency of DSSC study, a prepared TiO_2 photoanode with functioning area of 0.25cm^2 was immersed into 0.3mM of N719 dye for approximately 24h at room temperature. The platinum, Pt with mirror finished was fabricated by sputtering method and used as counter electrode. In order to complete the DSSC assembly, the electrolyte prepared from 1.59g of 1,2-dimethyl-3- propylimidazolium iodide, 10ml of iodolyte AN 50, 10ml of 4-tert-butylpyridine, 0.01g

of guanidine thio-cyanate and 5ml of valeronitrile was inserted in between both of the electrodes before clamped for measurement of solar cell (Ahmad, Soon, et al., 2016).

2.3 Characterization Techniques

The crystal structure of the as-synthesized films was examined by an X-ray diffraction (XRD) PANalytical X-Pert^3 Powder model with scan axis ranging from 20° to 70° with fixed divergence slit. The samples morphologies were observed by field emission scanning electron microscopy (FE-SEM, JOEL, JSM-7600F). The absorbance spectra were recorded in a range of 300nm - 800nm on a UV–Vis– NIR spectrophotometer (Shimadzu-UV 1800) to find the wavelength absorption. Four-terminal sensing measurement known as 4Point Probe (Signatone Pro4-440N) connected to source meter to determine the resistivity properties of the samples. The photovoltaic properties were quantified by a computer-programmed Kethley 2420 source meter under simulated AM1.5G irradiation by Newport Oriel solar simulator (100Mw/cm^2). The incident light intensity was calibrated with a reference Si solar cell.

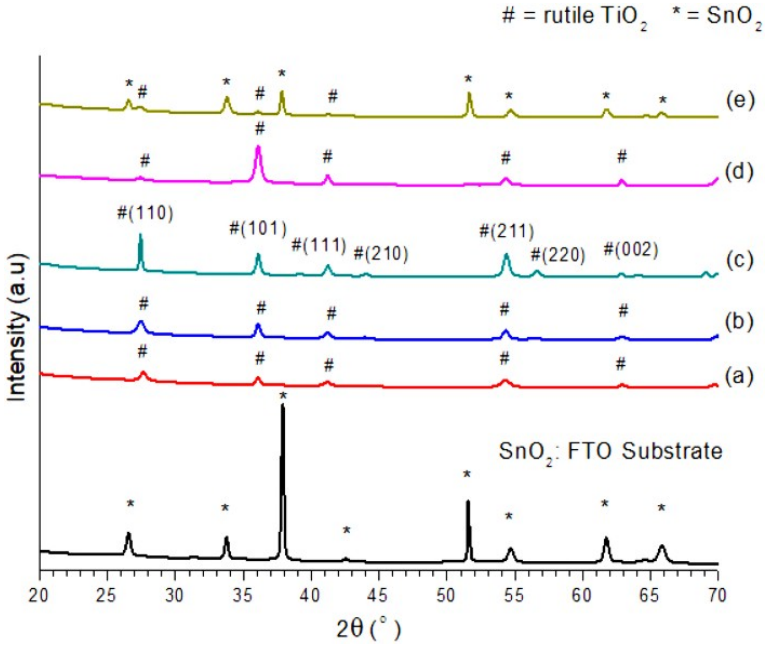

Fig. 1 - XRD pattern of FTO substrate and TiO2 thin film samples (a) TiO_2-HC50; (b) TiO_2-HC70; (c) TiO_2-HC80; (d) TiO_2-HC90; and (e) TiO_2-HC110

3. Results and Discussion

3.1 Structural Analysis

Fig. 1 demonstrates the evolution of XRD pattern of TiO_2 thin films prepared in various HCl volumes ranging from 50mL to 110mL on FTO substrate. As can be observed, all the samples prepared showed the prominent peak related to the rutile phase. For the sample TiO_2-HC50, there are five peaks of rutile were observed at 2θ = 27.3°, 36.1°, 41.3°, 54.4° and 63° reflected to (110), (101), (111), (211) and (002) planes. According to periodic bond chain of rutile lattice surface energy order, these facets are believed to have higher surface energy that promotes the nucleation process with fastest growth rate (Lin *et al.*, 2014). The broad shape of those peaks came out with a very weak intensity nature indicating a poor degree of crystallite thin film. No other peaks belong to SnO_2, anatase or brookite phase have been detected suggested a stability of thin film synthesized. Further increase of HCl volume can just increase the intensity of the peaks which show the improvement of the crystalline of the samples. Sample TiO_2-HC70 has similar number of rutile peaks as sample TiO_2-HC50. However, it can be seen clearly that the peaks for TiO_2-HC70 sample are apparently broad and quite weak in the intensity count of the film synthesis suggested that the nucleation rate has accelerated for nanorods and nanoflowers structure development.

Increasing the HCl volume to 80mL as denoted by TiO_2-HC80, the emergence of additional two peaks could be observed. Sample TiO_2-HC80 possesses seven rutile peaks indicating more TiO_2 nanostructures have been growth in various planes, consequently increase the crystallite of the prepared sample. These peaks are indexed to 2θ = 27.4°, 36.15°, 41.2°, 44.2°, 54.3°, 56.5° and 63.5° corresponding to (110), (101), (111), (210), (211), (220) and (002) with the strongest peak 135cts has been recorded at (110) facet as preferential plane.

To investigate the effect of HCl further additional, the volume has been increased to 90mL. Sample TiO_2-HC90 exhibits the significantly changes of the peaks growth. The peak growth at (210) and (220) facets were vanished and

leaving behind four rutile peaks indexed to 2θ = 36.15°, 41.2°, 54.3° and 62.5° corresponds to (101), (111), (211) and (002) planes with (101) as preferential plane due to the strongest peak obtained.

Table 1 - Structural parameters of prepared samples at different HCl concentrations

Sample	2θ (°)	Intensity (cts)	FWHM, β	Crystallite Size, D (nm)	Plane, (hkl)
TiO_2-HC50	27.33	40	0.246	39.83	110
TiO_2-HC70	27.36	123	0.295	69.26	110
TiO_2-HC80	27.42	135	0.147	69.27	110
TiO_2-HC90	36.15	165	0.394	39.63	101
TiO_2-HC110	36.10	64	0.295	32.67	101

However, when the volume of HCl is increased to 110mL denoted as TiO_2-HC110, only three rutile peaks at 2θ = 27.4°, 36.1° and 41.2° corresponding to (110), (101) and (111) were detected with broad and weak intensity elucidates the low crystalline of TiO_2 growth. The rest of rutile peaks are vanished and leaving behind SnO_2 peaks as dominant peaks in this sample. An excessive HCl amount could retard the hydrolysis rate whereas the insufficient HCl volume could decelerate the nucleation growth. One possible reason is the Cl^- ions that could preferentially adsorb and inhibit the growth rate of (110) surfaces. Therefore, it could be proposed that inadequate or excessive of HCl volume is unbeneficial for TiO_2 thin film synthesis in this research.

The crystallite sizes of rutile phase at different HCl concentrations were calculated according to Scherer equation: $D = K\lambda / \beta \cos \theta$, where D is the crystal size; λ is the wavelength of the X-ray radiation (λ = 0.15406nm) for CuKα; K is constant and usually taken as 0.9; and β is the line width at half-maximum height (FWHM), and θ (theta) is half of the diffraction angle in radian. It can be observed that the crystallite sizes exhibit significant increment but gradually decrease as increasing the HCl concentration as shown in Table 1. From the result obtained, the optimum condition for complete crystallization of the prepared TiO_2 films suggested when the amount of HCl should be equal to the de-ionized water to obtain sharper with strong intensity indicating the higher degree of crystallite. In this case, the amount of HCl is 80mL which equal to the amount of DI water. However, the result may vary depending on the conditions state of the experiment, the amount of precursor used and the process or method involved. Therefore, it is very difficult to make comparison of the results regarding the literatures on the effect of HCl on TiO_2 structure as there are low in number specifically by using hydrothermal method. From the results obtained, it is suggested that the volume of HCl has strongly influence in the fabrication of TiO_2 crystalline structure and preferential planes.

3.2 Morphological Studies

The surface morphological of TiO_2 films under various HCl concentrations were observed by FESEM as shown in Fig. 2. From cauliflower to chrysanthemum flower to dandelion structures are apparently grow on the FTO surface indicating the use of HCl rendered various kind of hierarchical TiO_2 rutile phase and are in good agreement with the XRD results previously. The role HCl as catalyst and chemical corrosive agent for the formation of rutile phase at the same time induce defects on the surface for the origination of double layer structures (Ye *et al*., 2013). Moreover, the concentrations of HCl also determine the yielded polymorphs of synthesized TiO_2 whether anatase, rutile or brookite phases. In this work, high acidic medium specifically HCl (Jiang *et al*., 2006) with a concentration more than 3M is selected to fabricate a high purity of rutile phase as reported by Su and co-workers (Su *et al*., 2011).

The sample TiO_2-HC50 employed 4.7M of HCl has morphology as shown in Fig. 2 (a) and Fig. 2 (b). It is observed that the TiO_2 film composed of cauliflower structure comprised of numerous coalesced TiO_2 nanorods that agglomerate and sticks to each other closely. This kind of structure is similar in a work done by Lin and group when they used low concentration of HCl that was 4M (Lin *et al*., 2014). The reason why this structure is agglomerated possibly because of the high surface energy that TiO_2 molecule possessed favours the attractive forces to hold the molecules together thus eliminated the energy and promoted the agglomeration between the TiO_2 molecules (Azimi-Fouladi *et al*., 2018). The thickness of the TiO_2 film is estimated to be 36.91um as depicted in Fig. 2 (c). By increasing the amount of HCl to 70mL or approximately 5.5M of HCl concentration (TiO_2-HC70), the formation of nearly perfect double-layer TiO_2 structure constitutes of numerous nanorods and nanoflowers have been initiated as depicted in Fig. 2 (d) and Fig. 2 (e). Nevertheless, the nanoflowers are grown in single disperse and the nanorods are closely stick to each other. The thickness of synthesized TiO_2 structure is estimated to be 6.833μm as shown in Fig. 2 (f) and greatly decreased compared to the sample TiO_2-HC50.

As the amount of HCl is increased to an equal proportion of DI water as designated by the sample TiO_2-HC80, the double-layer composed of nanorods and nanoflowers structures exhibit significant changes as confirmed by Fig. 2(g) and Fig. 2 (h). The nanorods are well-aligned with FTO substrate with tetragonal surface structure and a gap between them has been developed. Meanwhile, the nanoflowers structures have densely grown with many step-edges at the top of their petals with diameter ranging from 300 to 400nm. The thickness of TiO_2-HC80 sample is slightly increased to 9.28μm as depicted by Fig. 2 (i). Further increasing the amount of HCl to 90mL or 6.5M usage of HCl (sample TiO_2-HC90), the

double-layer structure of nanorods and nanoflowers showed greatly changes. It was clearly seen that the nanoflowers structures were not well-developed and decreased in number as shown in Fig. 2 (j) and Fig. 2 (k). Whereby, the nanorods structures were in tetragonal shape epitaxially grown on the FTO substrate with a large gap between them have been developed.

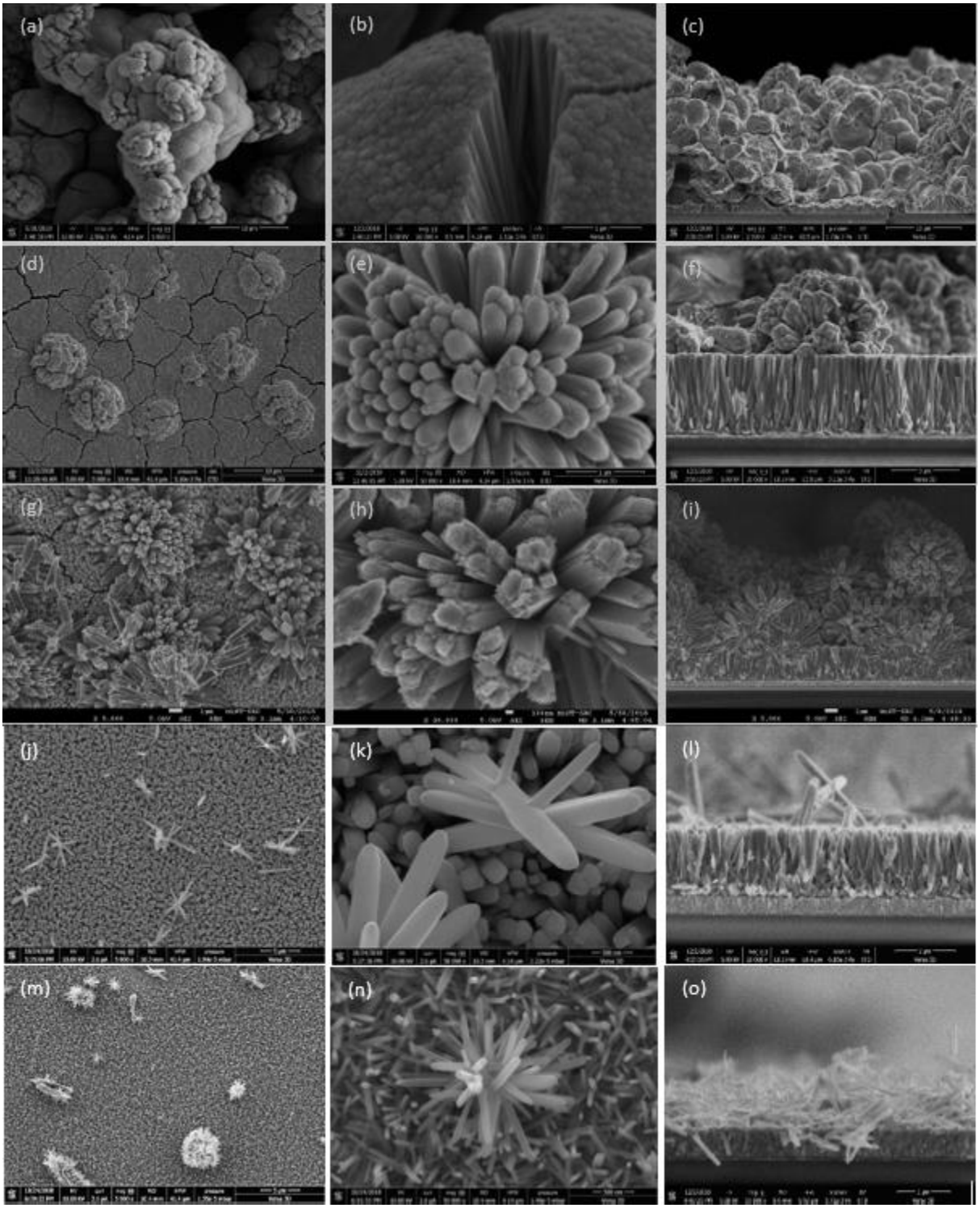

Fig. 2 - FESEM images of surface morphology of (a-b) TiO_2-HC50, (d-e) TiO_2-HC70, (g-h) TiO_2-HC80, (j-k) TiO_2-HC90 and (m-n) TiO_2-HC110 TiO_2 thin films at various magnifications and (c),(f),(i),(l),(o) cross-section view, respectively.

The nanorods diameters are slightly decreased approximately to 225-226nm and nanoflowers also reduced to ~310nm. In addition, the top of the nanoflowers are smooth served as a seed layer for TiO_2 to grow a bit longer. The thickness of TiO_2-HC90 sample is reduced abruptly and found to be 4.015µm as shown in Fig. 2 (l)**.** The experiment to

investigate excessive amount of HCl in TiO_2 nanostructures development has been conducted. The TiO_2-HC110 sample using 7M of HCl shows a great change to the TiO_2 nanostructure formed. It was seen clearly that the nanoflowers structures are not in well-formed and decrease in number as shown in Fig. 2 (m-n). This is suggested that too much HCl could inhibit the nanoflowers growth due to the highly OH^+ ions generated. The nanorods structures are in tetragonal shape inclined randomly grown on the FTO substrate with a larger gap between them. The diameter is slightly decreased approximate to 50-75nm and ~90nm for nanorods and nanoflowers, respectively. In addition, the top of the nanoflowers is possessed of many step edges and served as a seed layer for the subsequent growth of TiO_2. The thickness of TiO_2-HC110 sample is abruptly reduced and estimated around 1.359µm as shown in Fig. 2 (o).

All the outcomes indicate that the TiO_2 morphology could be adjusted by modifying the amount of HCl content. Furthermore, a moderate temperature during hydrothermal process may helpful in crystallization of TiO_2. According to Nguyen and co-workers, a low HCl concentration is primarily assigned to anatase phase formation with nanocubic particles structure (Nguyen *et al*., 2009). Whereas in a strong acidic medium, the rutile phase is built-up and can be found in many nanostructures such as flowers and rod-like morphologies. In fact, the abilities of several acid media to obtain a larger of TiO_2 particles have been investigated and HCl was identified as the strongest acidic solution when reacted with titanium butoxide as precursor (Wu *et al*., 2002). Hence, the result in this work is consistent with the previous literatures.

The formation of the crystalline phases either anatase or rutile is relied on the sharing mode and arrangement of basic structural unit of TiO_2 known as octahedron [TiO_6]. In a low amount of HCl, the number of OH ligands increased while the Cl^- ions possess a small number, there was a possibility of edge-shared bonding of octahedron that derived a formation of anatase phase. On the other hand, the increase of the HCl volume will reduce the OH ligands with chlorine ions become dense with a great number and promote easily the vertex-shared bonding rather than corner-shared and edge-shared bonding of the octahedron units to form a rutile phase (He et al., 2013). It was seen clearly that the growth of TiO_2 along the c-axis forming a prism or rod shape in rutile phase prior the anisotropic self-assembly of sub-units resulted the formation of cauliflower, chrysanthemum-flower or sea-urchin shape. But too much chloride ions which is negative ion could preferentially adsorb on positive polar of (110) surface and retard the crystal growth along the (001) plane. Thus, TiO_2 growth is suppressed on the [110] direction and accelerated in the [001] direction forming a prism or rod-like structure with small diameter and grew in randomly inclined direction (Ye *et al*., 2013) consistent with the XRD data, crystalline structure and preferential planes.

3.3 Optical Properties

Fig. 3 shows the UV-vis diffuse reflectance spectrum of the TiO_2 nanorods and nanoflowers double-layer structures. The absorption band edges were estimated around 420nm slightly higher than normally reported of λ = 388nm TiO_2. The intercept of the tangent to the plot versus as gives a good approximation of the band gap energy for this indirect band gap material. It shows the decreasing behaviour for TiO_2 band gap nanostructures as the volumes or HCl concentrations are increasing. The band gap energies (E_g) of as-prepared TiO_2 film are found to be 3.0eV, 2.88eV, 2.75eV, 2.57eV and 2.6eV corresponded to sample TiO_2-HC50, TiO_2-HC70, TiO_2-HC80, TiO_2-HC90 and TiO_2-HC110, respectively. The band gap decreases with increasing particle size and the absorption edge is shifted to a higher energy with decreasing particle size. The band gap values validate the crystallite size results according to which smaller crystallite size due to high HCl volume should have larger band gap and large crystallite size should have smaller band gap when increasing the HCl volume of nanostructures.

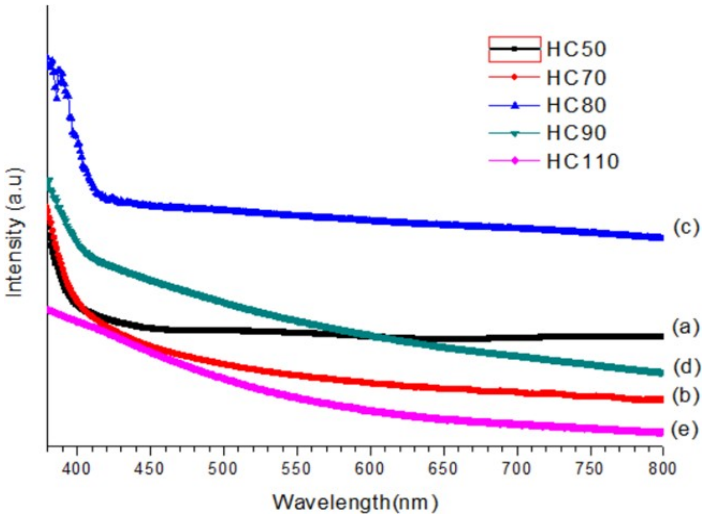

Fig. 3 - UV-Vis spectrometer of samples (a) TiO_2-HC50; (b) TiO_2-HC70; (c) TiO_2-HC80; (d) TiO_2-HC90; (e) TiO_2-HC110

3.4 Electrical Properties

Current-voltage (I-V) analysis was carried out and the result is depicted in Table 2. The amount of HCl affected the thickness of TiO_2 film where the thickness is decreased as the volume of HCl increased. The resistivity of nanorods or nanoflowers TiO_2 film growth shows a decreasing behaviour as the HCl has been increased from 50mL to 110mL. The enhancement of efficiency is further confirmed by IPCE measurements shown in Fig. 4. The variation of IPCE values at different HCl concentration follows the same trend as the efficiency variation. All the maximum IPCE peak values are in the wavelength range from around 300 to800nm. The maximum IPCE peak value of 42.5% corresponds to the DSSC with the TiO_2 synthesized using 80mL or 6M of HCl.

Table 2 - Electrical properties of as-prepared samples

Sample	Resistivity, R (Ω.cm)	TiO_2 thickness (um)
TiO_2-HC50	113.0	29.680
TiO_2-HC70	60.8	6.835
TiO_2-HC80	8.74	9.280
TiO_2-HC90	2.00	4.015
TiO_2-HC110	1.16	1.359

The increase in current density, J_{sc} up to this particular thickness is evidently related to the increase in injection current from excited dyes to the conduction band of TiO_2. As the adequate amount of HCl concentration, the maximum rate of photon absorption by the dye and the maximum rate of electron injection from the dye to the conduction band of TiO_2 evidently occur at this optimum concentration.

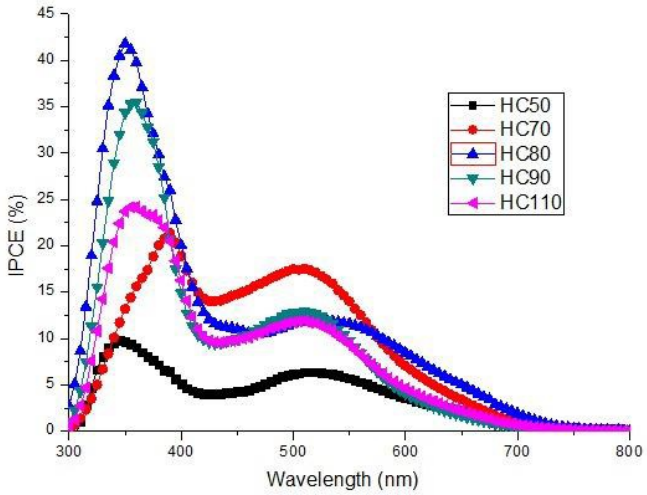

Fig. 4 - IPCE measurements of samples TiO_2-HC50, TiO_2-HC70, TiO_2-HC80, TiO_2-HC90 and TiO_2-HC110

The efficiency of the TiO_2 films is determined from the photocurrent-voltage characteristics are shown in Fig. 5 under a simulated sunlight at 100mW/cm^2. The details of the performances of the DSSCs are summarized in Table 3 for rutile phased photoanode. The density Jsc of rutile photoanode is increased with the conversion efficiency 6.41% of TiO_2-HC80 sample. An increase in the J_{sc} is the possible main cause for the increasing efficiency.

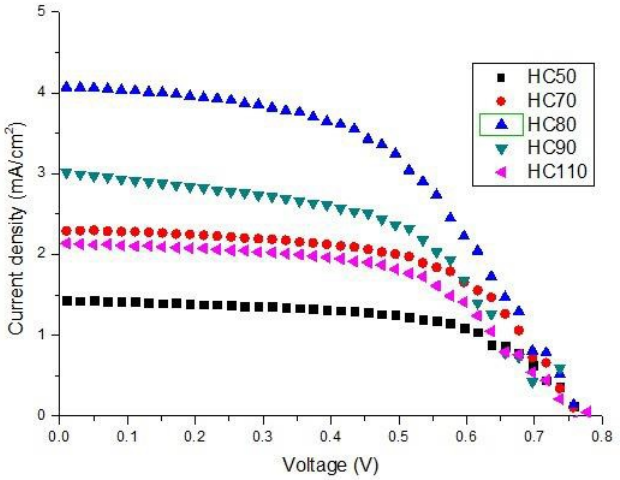

Fig. 5 - Current-voltage measurement of TiO_2 film

The current generated is determined by the amount of photoelectrons from the dye molecules. Higher amount of dye molecules naturally will generate more photoelectrons. The amount of dye molecules adsorbed onto the TiO_2 can be influenced by the surface area and the height of the nanorods and nanoflower of the TiO_2 samples.

Table 3 - Photovoltaic parameters of TiO_2 film

Sample (TiO_2-)	V_{oc} (V)	Jsc (mA/cm^2)	FF	η (%)
HC50	0.7608	5.7646	60.02	2.63
HC70	0.7545	9.1695	59.64	4.11
HC80	0.7060	11.6475	77.98	6.41
HC90	0.7102	12.0727	55.37	4.75
HC110	0.7645	8.5514	56.28	3.68

4. Conclusion

TiO_2 thin films were successfully synthesized through one-step hydrothermal method on the FTO substrate. The result evidently suggested that preferred plane transition from [110] to [110] facets occurred as the HCl concentration is increased. It also can be concluded that the insufficient amount of HCl attributed to the agglomeration due to a high energy surface between the molecules. Whereas an excessive of HCl, more chloride ions could preferentially adsorb then tend to contribute in slower hydrolysis rate and retarding the growth of nanoflowers thus promoted to the decrement of thicknesses and diameter of the nanorods and nanoflowers. Higher efficiency of DSSC could be yielded in this work by using an equal proportion of deionized water and HCl volume which is 80mL or in 1:1 ratio for TiO_2 thin film synthesis.

Acknowledgement

This study was supported by Program Hadiah Latihan Persekutuan 2017/2018, funded by Ministry of High Education Malaysia. The facilities and chemicals were provided by Microelectronic and Nanotechnology – Shamsuddin Research Centre (MiNT-SRC) and Universiti Tun Hussein Onn Malaysia. The acknowledgement is also expressed for all the colleagues and expertise assistance from technical support team on this research project.

References

[1] Ahmad, M. K., Mokhtar, S. M., Soon, C. F., Nafarizal, N., Suriani, A. B., Mohamed, A., Murakami, K. (2016). Raman investigation of rutile-phased TiO_2 nanorods/nanoflowers with various reaction times using one step hydrothermal method. *Journal of Materials Science: Materials in Electronics*, *27*(8), 7920–7926.

[2] Ahmad, M. K., Soon, C. F., Nafarizal, N., Suriani, A. B., Mohamed, A., Mamat, M. H., Murakami, K. (2016). Effect of heat treatment to the rutile based dye sensitized solar cell. *Optik*, *127*(8), 4076–4079.

[3] Apátiga, L. M., Rubio, E., Rivera, E., & Castaño, V. M. (2006). Surface morphology of nanostructured anatase thin films prepared by pulsed liquid injection MOCVD. *Surface and Coatings Technology*, *201*(7 SPEC. ISS.), 4136–4138.

[4] Arier, Ü. Ö. A., & Tepehan, F. Z. (2011). Controlling the particle size of nanobrookite TiO_2 thin film. *Journal of*

Alloys and Compounds, *509*(32), 8262–8267.

[5] Azimi-Fouladi, A., Hassanzadeh-Tabrizi, S. A., & Saffar-Teluri, A. (2018). Sol-gel synthesis and characterization of TiO_2-CdO-Ag nanocomposite with superior photocatalytic efficiency. *Ceramics International*, *44*(4), 4292–4297.

[6] Cabral, K. P., Kurniawan, W., & Hinode, H. (2015). Three-dimensional sea urchin-like TiO_2 synthesized via facile hydrothermal method: Its properties and solar photocatalytic activity. *Journal of Environmental Chemical Engineering*, *3*(4), 2786–2796.

[7] Dhandayuthapani, T., Sivakumar, R., & Ilangovan, R. (2016). Growth of micro flower rutile TiO_2 films by chemical bath deposition technique: Study on the properties of structural, surface morphological, vibrational, optical and compositional. *Surfaces and Interfaces*, *4*, 59–68.

[8] Dhas, V., Muduli, S., Agarkar, S., Rana, A., Hannoyer, B., Banerjee, R., & Ogale, S. (2011). Enhanced DSSC performance with high surface area thin anatase TiO_2 nanoleaves. *Solar Energy*, *85*(6), 1213–1219.

[9] Francis, L., Sreekumaran Nair, A., Jose, R., Ramakrishna, S., Thavasi, V., & Marsano, E. (2011). Fabrication and characterization of dye-sensitized solar cells from rutile nanofibers and nanorods. *Energy*, *36*(1), 627–632.

[10] He, Z., Cai, Q., Fang, H., Situ, G., Qiu, J., Song, S., & Chen, J. (2013). Photocatalytic activity of TiO_2 containing anatase nanoparticles and rutile nanoflower structure consisting of nanorods. *Journal of Environmental Sciences (China)*, *25*(12), 2460–2468.

[11] Hossain, F. M., Evteev, A. V., Belova, I. V., Nowotny, J., & Murch, G. E. (2010). Electronic and optical properties of anatase TiO_2 nanotubes. *Computational Materials Science*, *48*(4), 854–858.

[12] Iacomi, F., Apetroaei, N., Calin, G., Zodieriu, G., Cazacu, M. M., Scarlat, C., Schoenes, J. (2007). Structure and surface morphology of Mn-implanted TiO_2. *Thin Solid Films*, *515*(16 SPEC. ISS.), 6402–6406.

[13] Jiang, B., Yin, H., Jiang, T., Jiang, Y., Feng, H., Chen, K., Wada, Y. (2006). Hydrothermal synthesis of rutile TiO_2 nanoparticles using hydroxyl and carboxyl group-containing organics as modifiers. *Materials Chemistry and Physics*, *98*(2–3), 231–235.

[14] Jithin, M., Saravanakumar, K., Ganesan, V., Reddy, V. R., Razad, P. M., Patidar, M. M., Patil, P. S. (2016). Growth, mechanism and properties of TiO_2 nanorods embedded nanopillar: Evidence of lattice orientation effect. *Materials Letters*, *42*(7), 145–153.

[15] Li, J., Lin, C. J., Lai, Y. K., & Du, R. G. (2010). Photogenerated cathodic protection of flower-like, nanostructured, N-doped TiO_2 film on stainless steel. *Surface and Coatings Technology*, *205*(2), 557–564.

[16] Li, Y., Guo, M., Zhang, M., & Wang, X. (2009). Hydrothermal synthesis and characterization of TiO_2 nanorod arrays on glass substrates. *Materials Research Bulletin*, *44*(6), 1232–1237.

[17] Lin, C.-P., Chen, H., Nakaruk, A., Koshy, P., & Sorrell, C. C. (2013). Effect of Annealing Temperature on the Photocatalytic Activity of TiO_2 Thin Films. *Energy Procedia*, *34*, 627–636.

[18] Lin, J., Heo, Y. U., Nattestad, A., Sun, Z., Wang, L., Kim, J. H., & Dou, S. X. (2014). 3D hierarchical rutile TiO_2 and metal-free organic sensitizer producing dye-sensitized solar cells 8.6% conversion efficiency. *Scientific Reports*, *4*, 1–8.

[19] Liu, B., & Aydil, E. S. (2009). Growth of oriented single-crystalline rutile TiO_2 nanorods on transparent conducting substrates for dye-sensitized solar cells. *Journal of the American Chemical Society*, *131*(11), 3985–3990.

[20] Liu, Q. J., Ran, Z., Liu, F. S., & Liu, Z. T. (2015). Phase transitions and mechanical stability of TiO_2 polymorphs under high pressure. *Journal of Alloys and Compounds*, *631*, 192–201.

[21] Maheswari, D., & Venkatachalam, P. (2015). Enhancing the performance of dye-sensitized solar cells based on organic dye sensitized TiO_2 nanoparticles/nanowires composite photoanodes with ionic liquid electrolyte. *Measurement*, *60*, 146–154.

[22] Manoharan, C and Sridhar, R. (2012). Physical properties of spray pyrolysed TiO_2 films. *International Journal of Recent Scientific Research*, *3*(9), 775–777.

[23] Nguyen Phan, T. D., Pham, H. D., Viet Cuong, T., Jung Kim, E., Kim, S., & Woo Shin, E. (2009). A simple hydrothermal preparation of TiO_2 nanomaterials using concentrated hydrochloric acid. *Journal of Crystal Growth*, *312*(1), 79–85.

[24] Nishanthi, S. T., Iyyapushpam, S., Sundarakannan, B., Subramanian, E., & Pathinettam Padiyan, D. (2014). Inter-relationship between extent of anatase crystalline phase and photocatalytic activity of TiO_2 nanotubes prepared by anodization and annealing method. *Separation and Purification Technology*, *131*, 102–107.

[25] Oja, I., Mere, A., Krunks, M., Nisumaa, R., Solterbeck, C. H., & Es-Souni, M. (2006). Structural and electrical characterization of TiO_2 films grown by spray pyrolysis. *Thin Solid Films*, *515*(2 SPEC. ISS.), 674–677.

[26] Pawar, U. T., Pawar, S. A., Kim, J. H., & Patil, P. S. (2016). Dye sensitized solar cells based on hydrothermally grown TiO_2 nanostars over nanorods. *Ceramics International*, *42*(7), 8038–8043.

[27] Senain, I., Nayan, N., & Saim, H. (2010). Structural and electrical properties of TiO_2 thin film derived from sol-gel method using titanium (IV) butoxide. *International Journal of Integrated Engineering*, (Issue on Electrical and Electronic Engineering), 29–35.

[28] Su, C., Chen, H. S., Chen, J. L., Yang, T. Y., Hsu, N. M., & Li, W. R. (2011). Preparation and characterization of pure rutile TiO_2 nanoparticles for photocatalytic study and thin films for dye-sensitized solar cells. *Journal of*

Nanomaterials, *2011*.
[29] Tighineanu, A., Ruff, T., Albu, S., Hahn, R., & Schmuki, P. (2010). Conductivity of TiO_2 nanotubes: Influence of annealing time and temperature. *Chemical Physics Letters*, *494*(4–6), 260–263.
[30] Vaiciulis, I., Girtan, M., Stanculescu, A., Leontie, L., Habelhames, F., & Antohe, S. (2012). On titanium oxide spray deposited thin films for solar cells applications. *Proceedings of the Romanian Academy Series A-Mathematics Physics Technical Sciences Information Science*, *13*(4), 335–342.
[31] Wang, Y., He, Y., Lai, Q., & Fan, M. (2014). Review of the progress in preparing nano TiO_2: An important environmental engineering material. *Journal of Environmental Sciences*, *26*(11), 2139–2177.
[32] Wang, Y., Wang, C., Zhang, X., Sun, P., Kong, L., Wei, Y., Liu, Y. (2014). TiO_2(B) nanosheets mediate phase selective synthesis of TiO_2 nanostructured photocatalyst. *Applied Surface Science*, *292*, 937–943.
[33] Wu, M., Lin, G., Chen, D., Wang, G., He, D., Feng, S., & Xu, R. (2002). Sol-hydrothermal synthesis and hydrothermally structural evolution of nanocrystal titanium dioxide. *Chemistry of Materials*, *14*(5), 1974–1980.
[34] Ye, M., Liu, H. Y., Lin, C., & Lin, Z. (2013). Hierarchical rutile TiO_2 flower cluster-based high efficiency dye-sensitized solar cells via direct hydrothermal growth on conducting substrates. *Small*, *9*(2), 312–321.
[35] Yuxiang, L., Mei, Z., Min, G., & Xidong, W. (2010). Hydrothermal growth of well-aligned TiO_2 nanorod arrays: Dependence of morphology upon hydrothermal reaction conditions. *Rare Metals*, *29*(3), 286–291.
[36] Zou, Y., Tan, X., Yu, T., Li, Y., Shang, Q., & Wang, W. (2014). Synthesis and photocatalytic activity of chrysanthemum-like brookite TiO_2 nanostructures. *Materials Letters*, *132*, 182–185.